generated. However, IR data suggest that the acid comprises less than 10% of the product. The NMR spectrum also indicated the presence of trapped Bu_3SnCl. This fact accounts for the anomalously large and variable interlayer spacing found for 6. Powder XRD patterns showed three orders of 00*l* reflections with an interlayer spacing ranging from 24.7 to 15.1 Å, depending upon the amount of Bu_3SnCl trapped between the layers. Bu_3SnCl can be partially removed by washing the solid in refluxing toluene; however, even the 15.1-Å phase contains a significant amount of Bu_3SnCl. The appearance of two weight losses totalling ca. 45% in the TGA of 6 (15.1-Å phase) provided additional evidence that Bu_3SnCl was present in the compound. The first weight loss of 25.1% occurred at a midpoint temperature of 390 °C; the second loss of 20.1% occurred at 1025 °C. If Bu_3SnCl had been removed during the reaction or subsequent washing, the expected total weight loss for the ester would be ca. 27%.

Much of the above chemistry has also been carried out with other members of the layered carboxylic acid zirconium phosphonate family—$Zr(O_3P(CH_2)_nCOOH)_2$. To date, we have been unable to prepare pure phases of Zr-$(O_3PCH_2COCl)_2$ and $Zr(O_3P(CH_2)_3COCl)_2$. It may be that the reactivity of $Zr(O_3P(CH_2)_nCOOH)_2$ is related to structural and/or electronic changes in the carboxylic acid region. For example, the orientation of the pendant acid group relative to the inorganic layers is expected to change as a function of the number of methylene spacers (n = odd or even number) between phosphorus and the acid group. We are currently addressing this structure–reactivity question through more detailed intercalation studies and with multinuclear NMR spectroscopy.

Conclusion

By and large the intercalation of organic guests into inorganic hosts have been promoted by only three types of reactions: acid/base, ion exchange, and redox. By use of functionalized group 4 metal phosphonates it is possible to employ other reactions, common in organic chemistry, to promote intercalation. Here we reported the synthesis of amides and esters from an acid chloride derivative. These materials are well ordered, thermally stable, and easily characterized. The wide range of functional groups available in these metal phosphonates suggests that our syntheses of amides and esters may be only the first examples of a large number of novel organic reactions that will promote the intercalation of organic molecules into layered inorganic solids.

Fourier Transform Infrared Spectroscopic Study of Predeposition Reactions in Metalloorganic Chemical Vapor Deposition of Gallium Nitride

B. S. Sywe, J. R. Schlup, and J. H. Edgar*

Department of Chemical Engineering, Durland Hall, Kansas State University, Manhattan, Kansas 66506-5102

The predeposition reactions that occur during metalloorganic chemical vapor deposition (MOCVD) of gallium nitride (GaN) were studied with Fourier transform infrared (FTIR) spectroscopy. The reactants studied included trimethylgallium (TMGa), ammonia (NH_3), and nitrogen trifluoride (NF_3). At room temperature, the predeposition reaction between TMGa and NH_3 went to completion immediately after mixing. The resulting adduct, $TMGa:NH_3$, was easily observed in the gas phase via FTIR spectroscopy. Assignments have been made to the IR absorption bands of gaseous $TMGa:NH_3$. At 150 °C, chemical equilibrium was reached between the gaseous adduct, $TMGa:NH_3$, and the reactants. The forward rate constant of this predeposition reaction is 5.89×10^{-3} (Torr s)$^{-1}$. No evidence of gas-phase adduct formation was observed when NF_3 was mixed with TMGa at room temperature and at 150 °C. This suggests a potential advantage of NF_3 over NH_3 as a nitrogen source in MOCVD of GaN.

Introduction

In the past two decades, metalloorganic chemical vapor deposition (MOCVD) has become one of the most widely used thin-film growth techniques for producing a complete range of III–V and II–VI compound semiconductor materials because of its technical simplicity and flexibility.[1-4] The MOCVD process is typically accomplished by the reaction of reactive metal–alkyls with a hydride of the nonmetal component. However, these precursors are very susceptible to forming adducts, even at room temperature, because metal–alkyls act as Lewis acids and the hydrides act as Lewis bases.[2] Thus, a difficulty commonly encountered in MOCVD processing of several compound semiconductors is the room-temperature predeposition of a nonvolatile adduct when the gaseous hydride is mixed with the metalloorganic vapor. Formation of nonvolatile adducts makes reliable transport of the reactants to the deposition zone difficult; thus precise control of both the

---

(1) Leys, M. R. *Chemtronics* 1987, 2, 155.
(2) Ludowise, M. J. *J. Appl. Phys.* 1985, 58, R31.
(3) Razeghi, M. *The MOCVD Challenge*; Adam Hilger: Philadelphia, PA, 1989; Vol. 1, p 9.
(4) Stringfellow, G. B. *Organometallic Vapor-Phase Epitaxy: Theory and Practice*; Academic Press: San Diego, CA, 1989; p 6.

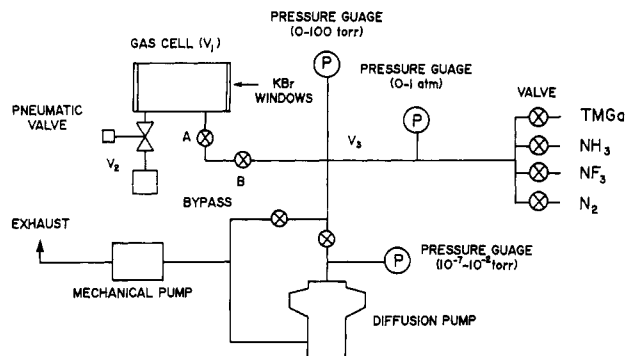*To whom correspondence should be addressed.

Figure 1. Schematic of the gas handling system used to transfer the precursors into the gas cell.

thickness and compositional uniformity of the epitaxial layer becomes unobtainable.

One MOCVD system that suffers from predeposition reactions is the deposition of gallium nitride (GaN) using trimethylgallium (TMGa) and ammonia (NH_3) as the source materials. GaN is a direct wide (3.45 eV) energy bandgap semiconductor with a high thermal conductivity. Potential device applications include high-frequency power switching devices and short-wavelength optoelectronic devices.[5] In MOCVD of GaN, NH_3 has long been used as the nitrogen source. Two problems are present when using NH_3: First, the uniformity of the deposited layer is poor because of the predeposition reaction between NH_3 and TMGa at room temperature. Second, the deposition temperature is high (greater than 800 °C) as a consequence of the thermal stability of NH_3.[6] Thus, there have been numerous attempts to find alternative nitrogen sources.[6-11] One reactant reported to have a low deposition temperature (440 °C) is nitrogen trifluoride (NF_3),[11] which has a lower bond energy (277 kJ/mol) as compared to NH_3 (391 kJ/mol). In addition, NF_3 is a nonpolar molecule with smaller dipole moment (0.234 D as compared with 1.42 D for NH_3),[12] which will help in reducing the extent of the predeposition reaction.

In this work, the predeposition reactions in MOCVD of GaN have been studied by in situ Fourier transform infrared (FTIR) spectroscopy. The reagents studied included TMGa (the most common Ga source), NH_3 (the most common nitrogen source), and NF_3 (a potential alternative source of nitrogen). With FTIR spectroscopy, both the identification of reaction products and quantitative analysis were possible.

Experimental Section

A Mattson Nova Cygnus 120 FTIR spectrometer with a germanium-coated KBr beamsplitter and a wide-range MCT (mercury-cadmium-telluride) detector was used to collect the infrared spectra. The spectral region measured was from 400 to 4000 cm^{-1}. The resolution was 4 cm^{-1}.

(5) Davis, R. F.; Sitar, Z.; Williams, B. E.; Kong, H. S.; Kim, H. J.; Palmour, J. W.; Edmond, J. A.; Ryu, J.; Glass, J. T.; Carter, C. H., Jr. *Mater. Sci. Eng.*, **1988**, *B1*, 77.

(6) Gaskill, D. K.; Bottka, N.; Lin, M. C. *Appl. Phys. Lett.* **1986**, *48*, 1449.

(7) Gaskill, D. K.; Bottka, N.; Lin, M. C. *J. Cryst. Growth* **1986**, *77*, 418.

(8) Mizuta, M.; Fujieda, S.; Matsumoto, Y.; Kawamura, T. *Jpn. J. Appl. Phys.* **1986**, *25*, L945.

(9) Fujieda, S.; Mizuta, M.; Matsumoto, Y. *Jpn. J. Appl. Phys.* **1987**, *26*, 2067.

(10) Kouvetakis, J.; Beach, D. B. *Chem. Mater.* **1989**, *1*, 476.

(11) Furukawa, Y. *Jpn. J. Appl. Phys.* **1984**, *23*, 376.

(12) Emeleus, H. J.; Shreeve, J. M.; Verma, R. D. *The Nitrogen Fluorides and Some Related Compounds*; *Advances in Inorganic Chemistry*; Sykes, A. G., Ed.; Academic Press: San Diego, CA, 1989; Vol. 33, pp 139–196.

A schematic of the gas handling system used to transfer the precursors into the gas cell is presented in Figure 1. The gas cell was constructed of stainless steel with KBr windows. This cell is comprised of a main body (V_1) and a small chamber (V_2), which are connected by a pneumatic valve. The main body has an i.d. of 26 mm, an o.d. of 32 mm, and an overall length of 10 cm. The volume ratio of the main body (V_1) to the small chamber (V_2) is 19.1. At the center of the outer surface of the cell body, a type K thermocouple was placed to monitor the cell temperature. Resistance heating tape wound evenly along the main cell body was used as a heat source. The cell temperature was controlled by a proportional controller. The upper operating temperature of the gas cell was 200 °C (limited by the Viton O-rings). Both a mechanical pump and a diffusion pump were used to evacuate the gas handling system. Electronic grade TMGa (99.99983%) was stored in a stainless steel bubbler as delivered from the supplier at room temperature. To remove any possible gaseous contaminants, the TMGa was frozen in the bubbler by using dry ice and the remaining gas was evacuated. The dry ice was removed, and the solid TMGa was melted. This process was repeated several times before the TMGa was used as a reagent. The other reagents included anhydrous NH_3 (99.99%), high-purity NF_3 (99.995%), and N_2 (99.995%), which were used as received.

Before introduction of any reactant into the cell, the gas cell and the manifold close to the cell (V_3) were baked out at 150 °C under continuous evacuation (to a pressure of ~2 × 10⁻⁶ Torr) for at least 12 h to remove any residual H_2O adsorbed on the inner surface of the tubing. After that, TMGa was loaded into the small chamber, and the cell body and the manifold were purged by alternately filling and evacuating with nitrogen several times. Then NH_3 or NF_3 was loaded into the cell body. The gas cell was disconnected from the gas handling system and placed in the FTIR sample compartment for data acquisition. The compartment was purged with dry air for 15 min to remove water vapor and CO_2 while heating the cell to the desired temperature. Then a reference interferogram of the NH_3 or NF_3 was collected. Once the reference spectrum had been obtained, the pneumatic valve was triggered to allow the TMGa in the small chamber to expand into the cell body. The kinetics of the predeposition reactions were monitored by obtaining the interferograms periodically after mixing.

Once the experiment was complete, the gas cell was removed from the spectrometer sample compartment and connected to the gas handling system. After pumping down to the background pressure (~2 × 10⁻⁶ Torr), the gas cell was put into the FTIR sample compartment again. An interferogram was collected after purging for 15 min. This interferogram served as the background for all the sample interferograms that had been collected previously. These sample and background interferograms were Fourier transformed to obtain the infrared spectra of the gas mixture.

The IR spectra of individual components were collected for compound identification. Calibration curves between the absorptions and the partial pressures of individual components were constructed for future quantitative analysis. The partial pressures of all components were less than 10 Torr, and no carrier gas was used.

Beside the IR studies, supplemental experiments were conducted to measure the volatility of the resulting adduct. These experiments were carried out by mixing the reactants in a constant volume reactor and recording the change in pressure after mixing. The constant volume reactor was composed of the main body of the gas cell (V_1) and the stainless steel tubings (V_3) in the gas handling system (Figure 1).

Results and Discussions

Figure 2 shows the IR absorption spectra of (a) TMGa, (b) NH_3, and (c) NF_3 in the gas phase at room temperature. The most characteristic absorption of TMGa appears at 583 cm^{-1}, corresponding to the Ga–C asymmetric stretching.[13] In addition, there are two strong absorptions at 2999 and 2917 cm^{-1} in the C–H stretching region. The ab-

(13) Kurbakova, A. P.; Leimes, L. A.; Aleksnyan, V. T.; Golubinskaya, L. M.; Zorina, E. N.; Bregadze, V. I. *Zh. Strukt. Khim.* **1974**, *15*, 1083.
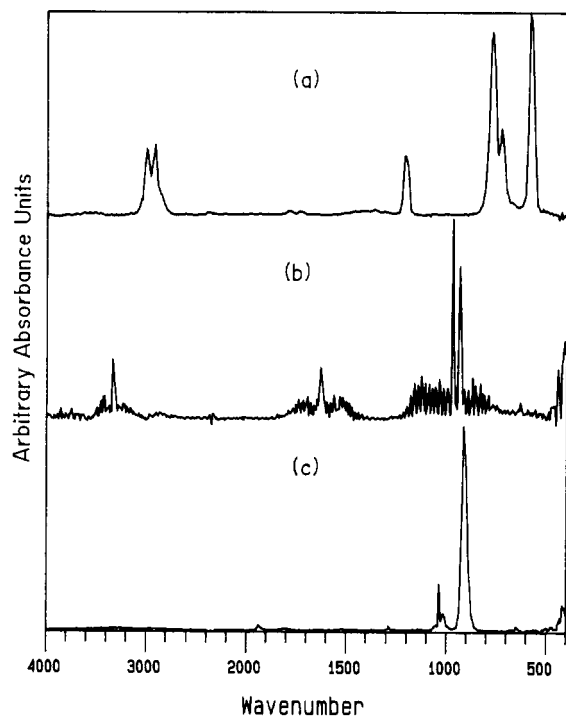
Figure 2. Infrared absorption spectra of (a) TMGa, (b) NH_3, and (c) NF_3 at room temperature.

sorption bands at 1210, 1206, and 1198 cm⁻¹ result from CH_3 symmetric deformations. The strong peak at 771 cm⁻¹ with a shoulder at 725 cm⁻¹ is attributed to CH_3 rocking modes. NH_3 has absorptions at 3333, 1625, 965, and 931 cm⁻¹, corresponding to N–H symmetric stretching, asymmetric bending, and symmetric bending (965 and 931 cm⁻¹), respectively.[14] The vibrational–rotational structure is easily seen in NH_3 spectrum, even at 4-cm⁻¹ resolution. NF_3 has strong absorptions at 1031 and 909 cm⁻¹, corresponding to N–F stretching and deformation, respectively.[12] The Ga–C peak of TMGa at 583 cm⁻¹ and the intense peaks at 965 and 909 cm⁻¹ for NH_3 and NF_3, respectively, were selected as the analytical peaks for quantitative analysis.

Figure 3 shows the IR absorption spectra of (a) TMGa + NH_3 at room temperature with TMGa in excess, (b) TMGa + NH_3 at room temperature with NH_3 in excess, and (c) TMGa + NH_3 at 150 °C with NH_3 in excess. In the room-temperature spectrum of the mixture with TMGa in excess (Figure 3a), the complete disappearance of the NH_3 peaks is evident. NH_3 was totally consumed by forming an adduct with TMGa (TMGa:NH_3). The spectrum has features found in the pure TMGa spectrum; however, several significant differences exist. First, a very strong peak appears at 1136 cm⁻¹. Second, the line shape of C–H stretching peaks in the region 2800–3100 cm⁻¹ have changed. Third, the Ga–C peak of TMGa at 583 cm⁻¹ is still observed, but another peak appears at 569 cm⁻¹. Fourth, several weak peaks appear at 1590 cm⁻¹ and in the region between 3250 and 3500 cm⁻¹. Since TMGa is in excess (Figure 3a) and no NH_3 peaks are observed, this spectrum is a superposition of the spectra of pure TMGa and gaseous reaction products, most likely the adduct, TMGa:NH_3.

In the mixture spectrum at room temperature with NH_3 in excess (Figure 3b), the NH_3 peaks can be easily distinguished from other absorptions. Again, the first obser-
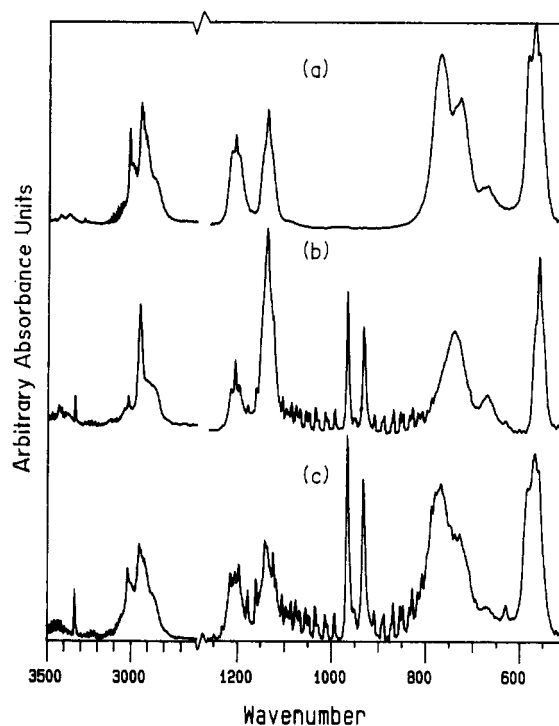

Figure 3. Infrared absorption spectra of (a) TMGa + NH_3 at room temperature with TMGa in excess, (b) TMGa + NH_3 at room temperature with NH_3 in excess, and (c) TMGa + NH_3 at 150 °C with NH_3 in excess.

vation is the appearance of the strong peak at 1136 cm⁻¹. Second, another strong peak appears at 2947 cm⁻¹ in the C–H stretching region. The TMGa peaks at 2999 and 2917 cm⁻¹ are not observed. Third, a new peak at 559 cm⁻¹ with a shoulder peak at 567 cm⁻¹ is observed, without the presence of the Ga–C peak of TMGa at 583 cm⁻¹. Fourth, in the C–H rocking region, the strong peak in the TMGa spectrum at 771 cm⁻¹ does not appear. Instead, a new peak at 739 cm⁻¹ is observed. Since NH_3 is in excess and all the characteristic peaks of TMGa are not observed in this spectrum, it is obvious that TMGa was exhausted by the adduct formation. From the correspondence of the new peaks in this spectrum to the pure TMGa spectrum, it can be concluded that this spectrum is a superposition of the spectra of pure NH_3 and the gaseous adduct TMGa:NH_3.

By examination of the two room-temperature mixture spectra (Figure 3a,b) in detail, absorption characteristic of TMGa:NH_3 can be distinguished from the TMGa and NH_3 peaks. The vibrational frequencies observed for gaseous TMGa:NH_3 are listed in Table I, along with those of TMGa and NH_3. The vibrational frequencies of solid TMGa:NH_3 and their assignments have been reported by Durig et al.[15] The assignments for the vibrational frequencies of gaseous TMGa:NH_3 were made by comparing the data herein to those of Durig et al. The Ga–N stretching absorption of TMGa:NH_3, which gives direct evidence of adduct formation, is expected to appear at approximately 368 cm⁻¹.[15] In the present study, this peak was not observed since far-infrared (<400 cm⁻¹) data were not obtained.

Figure 3c shows the spectrum of TMGa + NH_3 mixed at 150 °C with NH_3 in excess. Unlike the room-temperature spectrum in Figure 3b, the Ga–C peak of TMG at 583 cm⁻¹ is observed in this spectrum. In addition, absorptions for both NH_3 and TMGa:NH_3 are observed; this

(14) Tripathi, A.; Mazzarese, D.; Connor, W. C. *J. Electron. Mater.* **1989**, *18*, 45.

(15) Durig, J. R.; Bradley, C. B.; Odom, J. D. *Inorg. Chem.* **1982**, *21*, 1466.

Table I. Frequencies of the Normal Vibrations of NH₃, TMGa, and TMGa:NH₃ (cm⁻¹)

NH₃(g)	TMGa(g)	TMGa: NH₃(g)	TMGa: NH₃(s)[a]	assignment[b]
3432 vw[c]		3427 w	3350 s	NH₃ a str
3414 vw		3372 w	3277 m	NH₃ s str
3333 w		3284 w	3267	
	2999 s	2947 vs	2940 s	CH₃ a str
	2917 s		2882 m	
			2832 sh	CH₃ s str
1625 w		1590 m	1610 m	NH₃ a def
965 m		1203 s	1224 s	NH₃ s def
931 m			1207 s	
	1210 s			
	1206 sh	1136 vs	1177 vs	CH₃ s def
	1199 sh			
	771 vs	739 vs	750 vs	CH₃ in-plane rock
	725 s	669 m	723 s	
			709 s	CH₃ out-of-plane rock
	583 vs	567 sh		
	573 sh	559 vs	542 vs	Ga–C a str
			368 m	Ga–N str

[a] From Durig et al.[15] [b] Abbreviations for peak assignment: a = asymmetric, s = symmetric, str = stretching, def = deformation. [c] Abbreviations for relative peak intensity: vs = very strong, s = strong, m = medium, w = weak, vw = very weak, sh = shoulder.

spectrum is the superposition of the spectra of the gaseous product TMGa:NH₃ with pure reactants TMGa and NH₃. Therefore, while formation of adducts in the gas phase is observed at 150 °C, the reaction no longer favors complete consumption of the limiting reactant. An equilibrium between the individual reactants and product in the gas phase is reached.

From the pure-component IR spectra, the absorptions of an individual component at various pressures were correlated by assuming Beer's law. Accordingly, the partial pressure change of the reactants before and after mixing were calculated, yielding the amount of the reactants consumed. It is clear that the adduct formation from TMGa and NH₃ goes to completion at room temperature. Since it is possible that the product is distributed between the condensed phase and the gas phase, the equilibrium constant for the gas-phase reaction could not be determined.

In another experiment, TMGa was mixed with excess NH₃ at room temperature, and the temperature of the mixture raised to 150 °C. The spectra of this mixture at room temperature and at 150 °C are overlaid in Figure 4. Upon heating, several changes occurred in the spectra. First, the intensities of the TMGa:NH₃ peak at 1136 cm⁻¹ and the Ga–C peak of TMGa:NH₃ at 559 cm⁻¹ decreased. Second, the intensities of the NH₃ peaks increased and the Ga–C peak of TMGa at 583 cm⁻¹ appeared. Last, the TMGa:NH₃ peak at 739 cm⁻¹ became unobservable and the TMGa peak at 771 cm⁻¹ appeared. These observations are consistent with dissociation of TMGa:NH₃ upon heating. Once equilibrium was achieved in this experiment, the spectrum obtained at 150 °C is the same as the mixture spectrum at 150 °C in Figure 3c. Therefore, there must be an equilibrium between the gaseous product TMGa:NH₃ and the reactants TMGa and NH₃ at 150 °C.

In the room-temperature experiments between TMGa and NH₃, kinetic data could not be obtained because the reactions were complete immediately upon mixing. The spectra taken before and after mixing showed a stepwise change in the peak intensities of the preexisting NH₃. In the spectra taken periodically after mixing, no further changes were observed. Although the FTIR spectrometer has the ability to collect spectra much faster than the rate
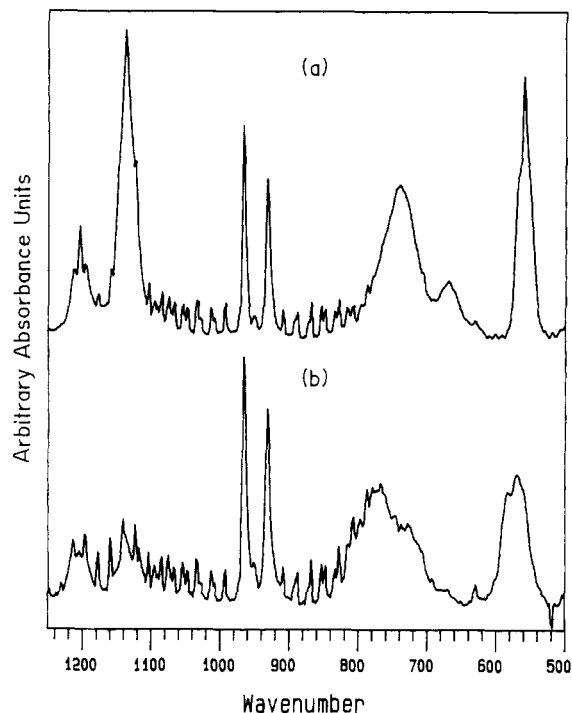

Figure 4. Infrared absorption spectra of TMGa + NH₃ (with NH₃ in excess), upon heating from (a) room temperature to (b) 150 °C.

used in this study, it is still difficult to determine the reaction rate at room temperature because the reaction rate would be limited by the mixing process. With use of an analog plotter to record the pressure change with time, it was estimated that the formation of TMGa:NH₃ was complete in less than 0.2 s at room temperature.

In the experiments at 150 °C, spectra taken periodically after mixing showed a continuous decrease in the peak intensities of TMGa and NH₃. The reaction reached chemical equilibrium in about 2 min. To interpret the kinetic data, the predeposition reaction between TMGa and NH₃ is assumed to be a reversible bimolecular reaction:

$$\text{TMGa(g)} + \text{NH}_3\text{(g)} \underset{k_2}{\overset{k_1}{\rightleftharpoons}} \text{TMGa:NH}_3\text{(g)} \qquad (1)$$
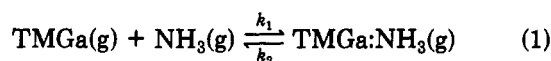
Assuming no product is present initially, the integrated rate equation below can be derived relating the conversion of NH₃ and time, t:

$$\ln\left[\frac{X_A - P_{B0}/(P_{A0}X_{Ae})}{X_A - X_{Ae}}\right] =$$
$$\ln\left[\frac{P_{B0}}{P_{A0}X_{Ae}^2}\right] + (P_{B0}/X_{Ae} - P_{A0}X_{Ae})k_1 t \quad (2)$$

where $X_A = (P_{A0} - P_A)/P_{A0}$ is the conversion of NH₃ at time t, X_{Ae} is the conversion of NH₃ at equilibrium, P_{A0} is the initial concentration of NH₃ in Torr at time = 0, P_{B0} is the initial concentration of TMGa in Torr at time = 0, k_1 is the rate constant for the forward reaction in (Torr s)⁻¹, and t is the reaction time in seconds.

From a plot of the logarithmic term of the left-hand side of eq 2 vs time, a straight line should be obtained with a slope equal to the forward rate constant k_1 times the constant term in the parentheses in the right-hand side. Figure 5 shows such a plot; the forward rate constant measured for TMGa + NH₃ at 150 °C is 5.89 × 10⁻³ (Torr s)⁻¹.
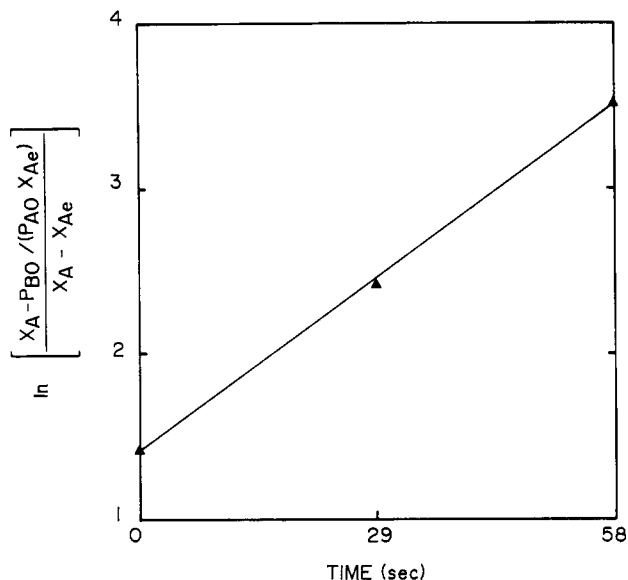
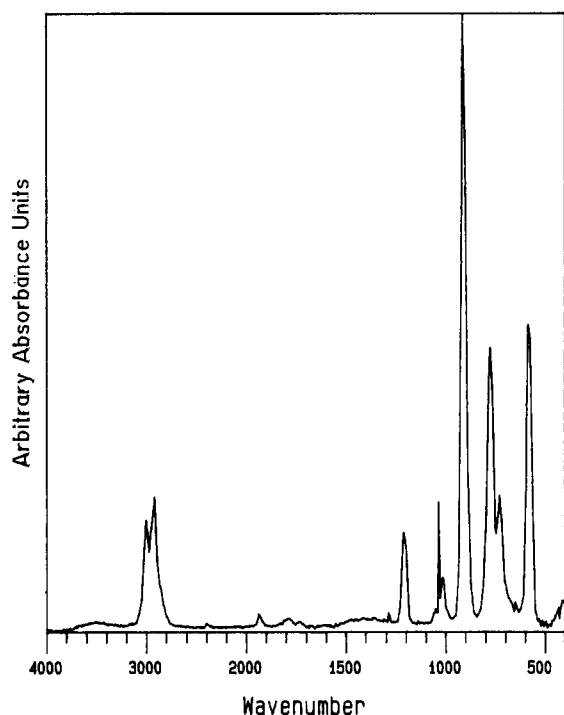**Figure 5.** Kinetic data for TMGa + NH_3 at 150 °C.

Figure 6. Infrared absorption spectra of TMGa + NF_3 at room temperature.

Figure 6 shows the spectrum of TMGa + NF_3 at room temperature. This spectrum is identical with the superposition of the pure-component spectra. The spectrum of TMGa + NF_3 at 150 °C is the same as the spectrum in Figure 6. The intensities of NF_3 peaks in both systems remain unchanged in 20 min. Therefore, no evidence of reaction was observed at either temperature.

The product of the predeposition reaction between TMGa and NH_3 previously has been described as a nonvolatile adduct with a melting point of 31–32 °C.[16] The present study has shown that a portion of these adducts remain in the gas phase and can be detected by IR spectroscopy using a gas transmission cell. However, the weak IR absorption of these adducts suggests most of the ad-

ducts are in a condensed phase. The data in Figure 4 indicate that these room-temperature adducts vaporize upon heating. An important question is the volatility of these adduct compounds at room temperature. To answer this question, some simple experiments were conducted by mixing the reactants in a constant volume reactor and recording the change in pressure following mixing. Furthermore, the reactivity of NF_3 toward TMGa was tested in these experiments also.

When NF_3 was mixed with TMGa, the total pressure after mixing was equivalent to the summation of the partial pressures of individual components; this indicates that no reaction occurred upon mixing at room temperature. This result is consistent with observations in the IR studies. In the TMGa + NH_3 system, the total pressure after mixing was intermediate between the sum and difference of the partial pressures of individual components. Since the IR data indicate that the reaction between TMGa and NH_3 goes to completion at room temperature, the pressure after mixing in excess of the difference between partial pressures of individual components was attributed to the vapor pressure of the adduct TMGa:NH_3 (assuming ideal gas behavior). The room-temperature vapor pressure of TMGa:NH_3 obtained varied from 0.46 to 1.37 Torr with an average of 0.92 Torr.

In the study of TMGa + NH_3 at 150 °C, the spectrum obtained 30 min after mixing exhibits an increase in the peak intensities associated with CH_4. The spectrum also shows decreases in the TMGa:NH_3 peaks, probably due to the condensation of the remaining complex, $(CH_3)_xGa:NH_x$, after the generation of CH_4. This is consistent with the result by Mazzarese et al.,[17] who reported the addition of NH_3 to TMGa accelerated the generation of CH_4. The subsequent elimination of CH_4 from TMGa:NH_3 could be a likely model in the MOCVD growth process of GaN using TMGa and NH_3, similar to the conclusion reached by Larsen et al.[18] for the MOCVD of GaAs using TMGa and AsH_3.

To eliminate the condensation predeposition adduct in the MOCVD process, one possible solution is to use a warm-wall reactor instead of a cold-wall reactor. For example, the wall temperature can be set at about 150 °C to reduce the predeposition reaction and to increase the vapor pressure of the adduct. Certainly, the optimal temperature will have to be determined experimentally. It must be much lower than the growth temperature to prevent deposition on the reactor wall.

From the aspect of limiting predeposition reactions, NF_3 is a good alternative nitrogen source since no evidence was obtained for the predeposition reaction between NF_3 and TMGa. However, fluorine has a higher chemical activity than nitrogen; thus, products containing fluorine may be formed in addition to the growth of the nitride semiconductor. For example, in MOCVD of AlN using TMAl and NF_3 as the source materials, aluminum trifluoride (AlF_3) was detected in the AlN films.[19]

Conclusions

The room-temperature predeposition reaction between TMGa and NH_3 is complete within 0.2 s following mixing. The resulting adduct had a vapor pressure that varied from 0.46 to 1.37 Torr. The IR absorption peaks of gaseous

(16) Andrews, J. E.; Littlejohn, M. A. *J. Eloectrochem. Soc.* **1975**, *122*, 1273.

(17) Mazzarese, D.; Tripathi, A.; Conner, W. C.; Jones, K. A.; Calderson, L.; Eckart, D. W. *J. Electron. Mater.* **1989**, *18*, 369.

(18) Larsen, C. A.; Buchan, N. I.; Stringfellow, G. B. *Appl. Phys. Lett.* **1988**, *52*, 480.

(19) Edgar, J. H.; Yu, Z. J.; Ahmed, A. U.; Rys, A. *Thin Solid Films* **1990**, *189*, L11.

TMGa:NH$_3$ were observed. The strongest absorption appears at 1136 cm^{-1}, corresponding to CH$_3$ symmetric deformation. The Ga–C stretching appears at 559 cm^{-1}, and the corresponding peak for TMGa appears at 583 cm^{-1}. When TMGa was mixed with NH$_3$ at 150 °C, chemical equilibrium was reached between the gaseous adduct TMGa:NH$_3$ and the reactants. By assuming reversible bimolecular reaction, a forward rate constant of 5.89 × 10^{-3} (Torr s)$^{-1}$ was measured for the predeposition reaction between TMGa and NH$_3$ at 150 °C. There was no evidence of a reaction between NF$_3$ and TMGa at either room temperature or 150 °C. Therefore, NF$_3$ could be used as an alternative source of nitrogen in order to limit predeposition reaction.

Phase Separation in Poly(enaminonitrile) Solutions and Blends

J. A. Moore,* Ji-Heung Kim, and Peter R. Seidel

Department of Chemistry, Polymer Science and Engineering Program, Rensselaer Polytechnic Institute, Troy, New York 12180-3590

The solubility behavior of poly(enaminonitrile) (PEAN) solutions and blends has been investigated by using light scattering. PEANs are soluble in a series of polyether solvents (glymes), and those solutions show cloud points as the temperature is raised. The same behavior was observed from miscible blends of PEAN with poly(ethylene oxide). Cloud points were determined by laser light scattering measurements.

Introduction

One of the more interesting aspects of miscible polymer blend studies is the finding that many of these systems show cloud points on heating. The equation-of-state theory that describes this behavior for small molecules also successfully interprets this behavior for a mixture of polymers with specific interactions (e.g., hydrogen bonding), leading to a negative heat of mixing.[1-6] Poly(enaminonitriles) (PEANs) are new high molecular weight, film-forming polymers that exhibit excellent thermal stability and good mechanical properties.[7] We have been studying blends of PEAN with several commercial polymers. It was found that PEAN forms miscible blends with good hydrogen-bond acceptors such as poly(ethylene oxide) (PEO), poly(4-vinylpyridine), poly(ethyloxazoline), and poly(*N*-vinylpyrrolidone).[8,9] Strong hydrogen bonding evidenced by FT-IR spectroscopy was suggested as the driving force that favors miscibility. The blends of PEAN with PEO showed particularly interesting lower critical solution temperature (LCST) type phase behavior. An endothermic transition associated with the phase separation was observed clearly by differential scanning calorimetry. In this article, we describe independent measurements of the cloud points of PEAN solutions in a series of polyether solvents (glymes) and polymer blends with PEO using the laser light scattering technique. Cloud point curves were established, which were in good accord with previous data.[9]

Experimental Section

Materials. PEANs were synthesized by using the procedure we developed for condensation polymerization of the chosen monomers with 4,4'-oxydianiline or 1,4-bis(4-aminophenoxy)-benzene in 1-methyl-2-pyrrolidinone (NMP) in the presence of DABCO as the acid acceptor.[7] Their structures and molecular characteristics are shown in Table I. A sample of 1,3-ODA–PEAN with intrinsic viscosity of 0.47 dL/g was found to have a weight-average molecular weight of 34 000 daltons by low-angle laser light scattering (LALLS). PEO with an average molecular weight of 100 000 daltons was purchased from Aldrich and used without purification. A series of ethylene glycol dimethyl ether (glyme) solvents (mono-, di-, tri-, and tetraglyme) was purchased from Aldrich. Penta-, hexa-, and heptaglyme were obtained from Parish Chemical Co. Poly(ethylene glycol) dimethyl ether samples with average molecular weights of 500 and 1000 daltons, were obtained from Hoechst Chemikalien. All glyme solvents were used as received without further purification.

Preparation of PEAN Solutions and Blends. The solutions were prepared by dissolving measured amounts of the polymers in glyme solvents and filtering through 0.45-μm microfilters. Blends were prepared by solution casting from DMF solutions. The solvent was evaporated slowly under N$_2$ flow at 60 °C. The resulting films were further dried in vacuo at 120 °C for 2 days and then slowly cooled to room temperature and stored in a

(1) Olabisi, O.; Robeson, L. M.; Shaw, M. T. *Polymer–Polymer Miscibility*; Academic Press: New York, 1979.
(2) Patterson, D.; Robard, A. *Macromolecules* 1978, *11*, 690.
(3) Saeki, S.; Kuwahara, N.; Konno, S.; Kaneko, M. *Macromolecules* 1973, *6*, 246.
(4) Paul, D. R.; Barlow, J. W. In *Multiphase Polymer*; Advance in Chemistry Series 176; American Chemical Society: Washington, DC, 1979; Chapter 17, p 315.
(5) Kwei, T. K.; Pearce, E. M.; Min, B. Y. *Macromolecules* 1985, *18*, 2326.
(6) Coleman, M. M.; Skroranek, D. J.; Painter, P. C. *Appl. Spectrosc.* 1984, *38*, 448.
(7) Moore, J. A.; Robello, D. R. *Macromolecules* 1989, *22*, 1084.
(8) Moore, J. A.; Kim, J.-H. *Proc. Polym. Mater. Sci. Eng. (Am. Chem. Soc.)* 1989, *61*, 679.
(9) Moore, J. A.; Kim, J.-H. *Polym. Prepr. (Am. Chem. Soc., Div. Polym. Chem.)* 1990, *31*, 696.